Magnetic resonance investigation of gold-doped and gold-hydrogen-doped silicon

P. T. Huy
Van der Waals–Zeeman Institute, University of Amsterdam, Valckenierstraat 65, NL-1018 XE Amsterdam, The Netherlands and International Training Institute for Materials Science, ITIMS Building, Dai hoc Bach khoa Hanoi, 1 Dai Co Viet Road, Hanoi, Vietnam

C. A. J. Ammerlaan
Van der Waals–Zeeman Institute, University of Amsterdam, Valckenierstraat 65, NL-1018 XE Amsterdam, The Netherlands

(Received 15 January 2002; revised manuscript received 30 April 2002; published 30 October 2002)

Three paramagnetic centers related to gold have been observed in gold-doped and gold-doped hydrogenated silicon by magnetic resonance. One spectrum, labeled Si-NL62, corresponding to a center with monoclinic-I symmetry, presents fourfold splitting due to the hyperfine interaction with one gold atom and further hyperfine interaction with two silicon nearest-neighbor atoms. After being diffused with hydrogen in a wet atmosphere of water vapor at 1300 °C for about 30 min, a second electron paramagnetic resonance spectrum, labeled Si-NL63, is detected, also of the monoclinic-I symmetry. The spectrum of the center is characterized by a complex hyperfine structure, in which, depending on magnetic field orientation, a sevenfold splitting with the intensities 1:2:3:4:3:2:1, a fourfold splitting 4:4:4:4, and other more arbitrary structures are observed. Extra small splitting is observed in the sample diffused with deuterium, indicating hydrogen involvement in the microscopic structure of the Si-NL63 center. Under band gap illumination the third center of a one-gold–two-hydrogen complex is observed. The center, labeled Si-NL64, has low triclinic symmetry and features the hyperfine interactions with one gold and two nearly equivalent hydrogen atoms. This results in a (1:2:1):(1:2:1):(1:2:1):(1:2:1) structure of each group of spectral lines. Spin-Hamiltonian parameters for the three spectra are determined and microscopic models are discussed.

DOI: 10.1103/PhysRevB.66.165219 PACS number(s): 61.72.Bb, 61.72.Tt, 76.30.He, 81.05.Cy

I. INTRODUCTION

Transition metals are important impurities in semiconductors, including silicon. When present in the materials, the transition metals create deep electronic levels within the band gap of the semiconductor, as a result of which the properties of the materials or devices are changed dramatically.

Gold in silicon is one of the most studied defects, due to its technological importance as carrier lifetime controller and its vital role in the understanding of the electronic properties of transition metals in a covalent host crystal. The amphoteric behavior of gold in silicon was clearly established.[1–3] Substitutional gold in silicon is known to introduce a deep acceptor level at $E_c - 0.54$ eV and a donor level at $E_v + 0.35$ eV.[4–6]

Transition metals are easily involved in impurity-pair or complex formation and in precipitation processes. A large variety of centers resulting from interaction of hydrogen with the transition metals Ti, Co, Ni, Cu, Ag, Pd, and Pt was observed using deep-level transient spectroscopy (DLTS).[7–16] Also, the interaction of hydrogen with gold in silicon has been investigated.[17–23] Using samples exposed to plasma between 150 and 350 °C, Pearton and Tavendale reported a substantial loss of the Au activity. No such effect was found, however, for samples annealed in hydrogen gas. Using the DLTS technique and a simple way of introducing hydrogen by wet chemical etching, Sveinbjörnsson *et al.* observed four deep levels, named G1–G4, in *n*- and *p*-type silicon. It was suggested that the G1, G2, and G4 levels are related to the same Au-H defect consisting of a single-gold–single-hydrogen pair. The G3 level was assigned to a Au-H_2 complex. Unfortunately, DLTS does not yield direct information about the microscopic structure or chemical composition of the defects. Magnetic resonance, capable of providing detailed insight into the structure of centers, has so far only been reported for the orthorhombic Pt-H_2 center and for the trigonal complex $(\text{Pt-H}_2)_3$ (spectrum Si-NL53).[24–25]

In the present study an effort has been made to elucidate the atomic and electronic structure of defects related to gold and gold-hydrogen complexes using electron paramagnetic resonance (EPR). We report on three EPR centers, which will be labeled Si-NL62, Si-NL63, and Si-NL64, and which, on the basis of the analysis of experimental observations, will be assigned to a single gold center, a gold-hydrogen complex, and a complex of Au-H_2, respectively.

II. EXPERIMENT

The material used in this experiment is silicon, either *p*-type float-zoned boron-doped with the room-temperature resistivity of 75–125 Ω cm or *n*-type Czochralski-grown phosphorus-doped single crystal with the resistivity in the range 0.75–1.25 Ω cm at room temperature. The crystals were oriented and cut into rectangular bars with the typical dimensions of $1.5 \times 1.5 \times 15$ mm^3, with the longest side parallel to a ⟨011⟩ crystallographic direction.

Gold and hydrogen were separately diffused into the samples in the following procedure. First, gold was introduced by thermal diffusion at a temperature between 1200 and 1300 °C for 2 h (set 1) or 12 h (set 2) from a thin layer covering one side of the sample and for 48 h (set 3) or 72 h (set 4) from a thicker layer on all surfaces of the sample in an

argon gas atmosphere. Diffusion was terminated by a quench into water at room temperature. A high diffusion temperature, fast quenching after diffusion, and high gold concentration were found to be requirements for the production of the paramagnetic centers. After the gold diffusion step, the gold-covered surface regions were mechanically removed and the samples were further cleaned by etching in a CP6 (HNO_3:HF:CH_3COOH=2:1:1) solution. Subsequently the samples were measured by EPR spectroscopy. For the diffusion of hydrogen, samples were again put into a quartz ampoule filled with argon gas and a few milligrams of pure or heavy water, and then heated to 1300 °C for about half an hour. Again, a quench in water at room temperature concludes the diffusion stage.

Magnetic resonance measurements were carried out with a superheterodyne spectrometer which is operated in the *K* band, i.e., with the microwave frequency near 23 GHz. Signals were observed with the spectrometer tuned to dispersion under conditions of adiabatic fast passage. The large static magnetic field could be swept linearly with time. To allow phase sensitive detection, a small magnetic field with an amplitude of approximately 0.1 mT and modulated at a frequency near 175 Hz was superimposed on the static field. Samples were mounted with their long side along the axis of the cylindrical microwave cavity resonating in the TE011 mode. The long sample edge is indicated as the [0,−1,1] crystal direction. The magnetic field can be rotated in the perpendicular horizontal (0,−1,1) plane. The spectrometer has an option of operation under full computer control.

III. MAGNETIC RESONANCE SPECTRA

A. EPR spectrum Si-NL62

In *n*-type gold-diffused samples quite strong signals covering a wide magnetic field range were observed. A typical spectrum recorded at a temperature of 4.2 K for magnetic field $\mathbf{B}\|[100]$ crystallographic direction of the sample is shown in Fig. 1. The spectrum is characterized by a prominent splitting into groups of four equal-intensity lines due to hyperfine interaction with a nuclear spin $I=\frac{3}{2}$ of a magnetic nucleus of 100% natural abundance. In addition, weaker spectral lines due to hyperfine interactions with silicon neighbor atoms are observable. For further reference this new spectrum is labeled Si-NL62. At the same time, a weaker signal of the well-known Au-Fe center is observed in the magnetic field region of 765 to 770 mT.[26–27] From the full angular dependence pattern upon rotation of magnetic field in the (0,−1,1) plane the monoclinic-I symmetry for the Si-NL62 center is concluded. Due to the strong anisotropy of the spectrum some splitting due to sample misorientation is almost unavoidable. For a misorientation of about 5°, as present in Fig. 2, all twelve orientations of the defect are distinguishable, actually providing an independent additional evidence for the monoclinic symmetry. The angular dependence of the four main lines of the spectrum is well described with electron spin $S=\frac{1}{2}$ and a nuclear spin $I=\frac{3}{2}$ by the Hamiltonian

$$H=\mu_B\mathbf{B}\cdot\mathbf{g}\cdot\mathbf{S}-g_n\mu_N\mathbf{B}\cdot\mathbf{I}+\mathbf{S}\cdot\mathbf{A}\cdot\mathbf{I}+\mathbf{I}\cdot\mathbf{Q}\cdot\mathbf{I}, \qquad (1)$$

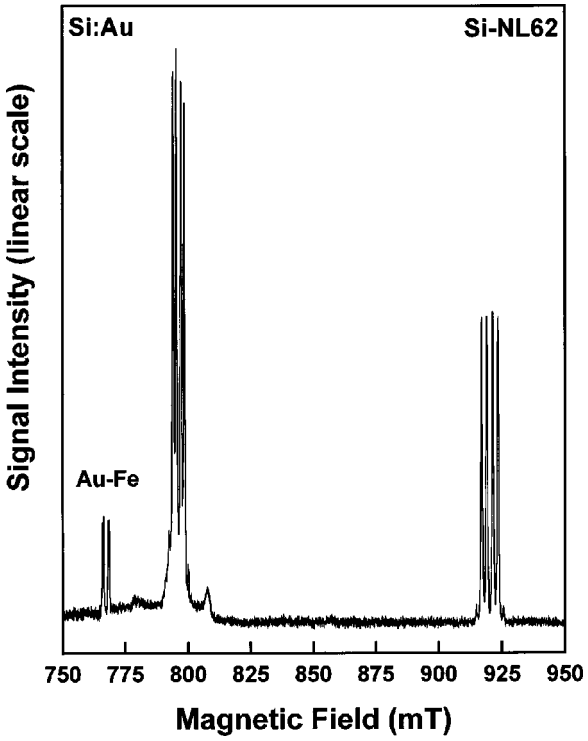

FIG. 1. Typical EPR spectrum of the Si-NL62 center observed in *n*-type gold-diffused silicon for magnetic field $\mathbf{B}\|[100]$, microwave frequency ν=22.7856 GHz, temperature $T=4.2$ K. Fourfold splitting due to hyperfine interaction with one gold atom, nuclear spin $I=\frac{3}{2}$, abundance 100%, is clearly observable. The EPR spectrum Si-A23 of the well-known Au-Fe pair is also present, as indicated.

in which **A** and **Q** represent hyperfine and quadrupole interaction tensors, respectively, related to the ^{197}Au isotope.

Previously, the analysis of gold-related EPR spectra has required the assumption of a large quadrupole effect,[28–30] even though it is a purely nuclear energy. A large quadrupole effect will cause an appreciable mixing of states, as a result of which different transitions become dominant in the electron spin resonance. Also for the Si-NL62 spectrum the quadrupole term has a strong effect on the spectrum as manifested by spectra recorded in the three principal directions of the **g** tensor. A spectrum recorded for the magnetic field parallel to the principal **g**-tensor direction [011] on orientations *bc* and *cb*, as shown in Fig. 3, reveals the quadrupole effect by the nonequidistance of the spectral components. By an analytical analysis of the eigenvalue problem of Eq. (1) in the regime of strong quadrupole effect compared to hyperfine effect, the separation ΔB of inner and outer pairs of lines in the spectra is obtained as

$$\Delta B=|A_1||1\pm 2/\{1+[(Q_2/Q_3)-1]^2/ 3[(Q_2/Q_3)+1]^2\}^{1/2}|/g_1\mu_B, \qquad (2)$$

and cyclic expressions in the principal values g_i, A_i, and Q_i of the **g**, **A**, and **Q** tensors, $i=1$, 2, and 3. In the derivation, the principal axes of **g**, **A**, and **Q** tensors were assumed to coincide. The positive sign refers to the outer doublet, the

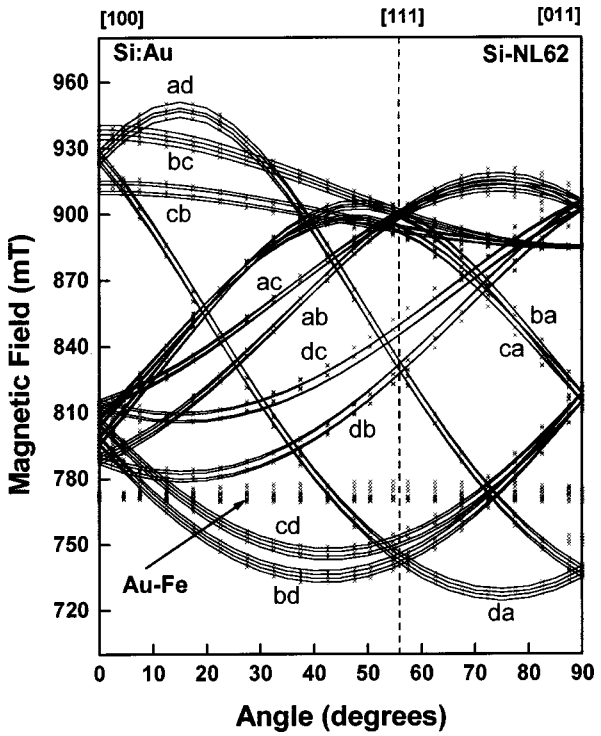

FIG. 2. Monoclinic-I angular dependence pattern of the Si-NL62 spectrum for rotation of the magnetic field in the $(0,-1,1)$ plane from [100] to [011]. Experimental data recorded at temperature $T=4.2$ K for microwave frequency $\nu=22.8155$ GHz are presented by $\times$. Solid lines are from the computer fit using the spin Hamiltonian of Eq. (1), with a sample misorientation of about 5°. Labeling of the defect orientations follows the convention as outlined in Ref. 53.

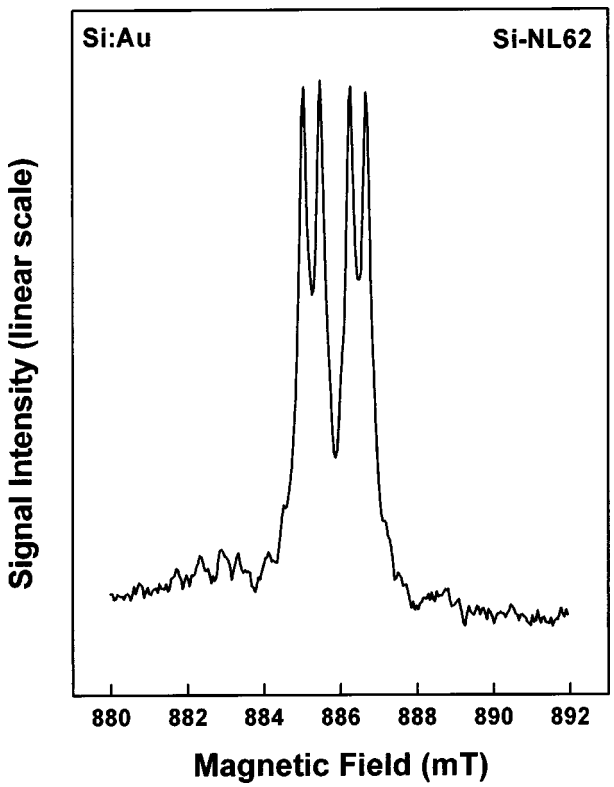

FIG. 3. EPR spectrum of center Si-NL62 recorded with magnetic field $\mathbf{B}\|[011]$, parallel to the principal direction of the **g** tensor on orientations *bc* and *cb*.

minus sign to the inner doublet. The result shows that ratios of quadrupole parameters are directly derived from the ratio of inner to outer pair splitting. An absolute value of quadrupole parameters cannot be obtained from the experimental data, only a lower limit of the Q parameter can be established. Once the ratios of the Q parameters are fixed, the hyperfine constants are calculated from the absolute values of the splittings using Eq. (2). For spectrum Si-NL62 the analysis is illustrated in Fig. 4. Following Eq. (2) the splitting of the inner pair is plotted with the positions of the lines of the outer pair normalized to unity. From the experimental field splittings the ratios of quadrupole parameters are obtained as $Q_2/Q_3=-1.23$, $Q_3/Q_1=+4.85$, and $Q_1/Q_2=-0.20$. These ratios are taken as input data for the numerical computer diagonalisation of Eq. (1) with the calculation of resonance fields. Spin-Hamiltonian parameters calculated from fitting the resonance fields are given in Table I. Principal values of the **Q** tensor are determined as $Q_1=+q$, $Q_2=-5.2q$, and $Q_3=+4.2q$, with $q>15$ MHz, as given in Table I. The average least-squares error of 10 μT is much smaller than the experimental uncertainty. There exists a remarkable similarity between the parameters of the Si-NL62 center and the only other monoclinic gold-related center, the C_{1h} center of Höhne.[29] One can notice a clear correspondence between the principal values of the **g**, **A**, and **Q** tensors, even if differences are several tenths of times outside experimental error and principal directions are interchanged.

In addition to gold, a hyperfine structure due to silicon neighbors was observed, as noticeable in Fig. 1. From the intensity of the weak lines it is concluded that two ^{29}Si neighbor nuclei on probably equivalent sites are involved. As

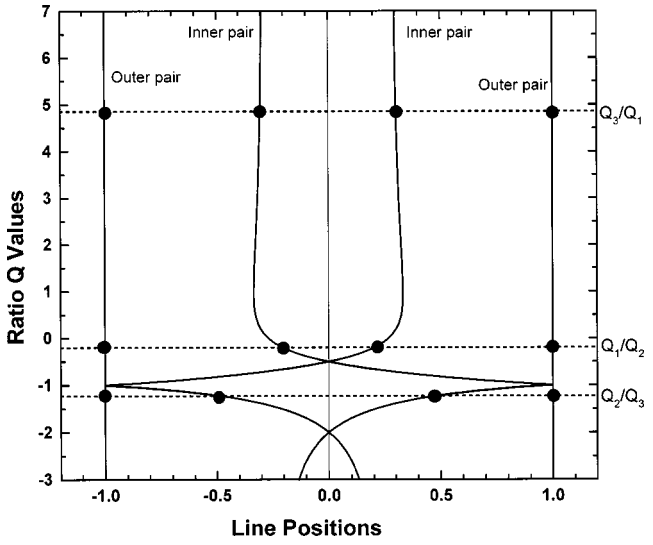

FIG. 4. Separation of the inner pair of resonance transitions as a fraction of outer pair line distance, as a function of the ratio of quadrupole tensor principal values Q_1, Q_2, and Q_3, calculated from Eq. (2) in text. Magnetic field is parallel to a principal axis of the **g**, **A**, and **Q** tensors, which are assumed to coincide. Fit of data for spectrum Si-NL62 indicated.

TABLE I. Spin-Hamiltonian parameters for the spectra Si-NL62, Si-NL63, and Si-NL64, following from analysis by Eqs. (1) and (3). All centers are described by electron spin $S=\frac{1}{2}$. For the monoclinic centers, the direction labeled 1 is parallel to [011], direction 3 is inclined against [100] by an angle θ (degrees).

Parameter	$g_1/A_1/Q_1$	$g_2/A_2/Q_2$	$g_3/A_3/Q_3$		θ	Units
Spectrum Si-NL62—Symmetry monoclinic-I						
g	1.8424	2.2435	1.7165		15	
$\mathbf{A}^{\mathrm{Au}}$	(−) 31.4	(+) 57.5	(−) 65.7		15	MHz
$\mathbf{Q}^{\mathrm{Au}}$	$+q$	$-5.2q$	$+4.2q$	$\lvert q\rvert>15$	15	MHz
$A^{\mathrm{Si}}_{[100]}$	110					MHz
Spectrum Si-NL63—Symmetry monoclinic-I						
g	1.9138	2.2942	2.0387		21	
$\lvert\mathbf{A}^{\mathrm{Au}}\rvert$	34.5	46.8	42.2		10	MHz
Spectrum Si-NL64—Symmetry triclinic						
g	$g_{xx}=2.1282$	$g_{yy}=2.0690$	$g_{zz}=2.0039$			
	$g_{xy}=-0.0732$	$g_{yz}=0.0394$	$g_{zx}=0.0361$			
$\lvert\mathbf{A}^{\mathrm{Au}}\rvert$	$A_{xx}=13.8$	$A_{yy}=23.5$	$A_{zz}=18.1$			MHz
	$A_{xy}=8.72$	$A_{yz}=-6.36$	$A_{zx}=1.06$			MHz
$\mathbf{A}^{\mathrm{H}}$	$A_{xx}=8.68$	$A_{yy}=11.39$	$A_{zz}=8.54$			MHz
	$A_{xy}=1.73$	$A_{yz}=-0.24$	$A_{zx}=0.14$			MHz

the resonances are close to the gold structure, the angular dependence could not well be followed. Only the value in the $\mathbf{B}\|[100]$ direction could be measured and is given in Table I.

No other hyperfine structure was revealed in the EPR spectra. A conclusion toward a single isolated gold atom is, however, unlikely as it has been shown that the gold center has tetragonal symmetry and is unobservable in EPR due to its vanishing perpendicular g value.[31] Since in the same sample the Au-Fe pair appeared to be present, the involvement of other transition element impurities in the Si-NL62 center has been examined. In additional experiments with the introduction of copper, silver, iron, and other $3d$ impurities, with or without gold codoping, the Si-NL62 spectrum was not observed.

In the starting *n*-type material the phosphorus EPR spectrum is strongly present, but no trace of it is left after the diffusion with gold. This hints at an electron capture of the Si-NL62 center, becoming paramagnetic in a possibly negative charge state. Consistent with this observation, the gold diffusion in the boron-doped *p*-type floating-zone silicon gave neither the Si-NL62 spectrum nor other gold-related signals. However, right after the hydrogen-doping treatment, the Si-NL62 spectrum, and the Au-Fe spectrum as well, are observed in all samples. A role of hydrogen in the formation of the centers is thus indicated. As the monoclinic symmetry of the Si-NL62 center indicates a complex core, a direct involvement of hydrogen as a constituent of the center is suggested. As this possibility is not supported by observed hydrogen hyperfine structure, the thermal stability of the assumed gold-hydrogen complex has been studied by isochronal anneal. Samples were enclosed in ampoules with argon gas at 200 mbar and annealed at temperatures in the range 100 to 650 °C, with temperature increments of 20 °C, for durations from 1 to 2 h. The Au-Fe pair is lost by dissociation after 520 °C/1 h annealing. The Si-NL62 center is observable under normal measurement conditions until 580 °C. At this temperature the EPR spectrum of phosphorus becomes weakly detectable and the Si-NL62 spectrum requires visible-light illumination. After annealing at 600 °C the P spectrum has recovered to its original doping concentration, but Si-NL62 remains visible under illumination. After 650 °C annealing for two hours the Si-NL62 signal has disappeared without creating any new center. The Si-NL62 center has a remarkable thermal stability, in contrast to established hydrogen-complex centers.[32]

While the Si-NL62 spectrum is observed in all gold-diffused samples, its strength varies between the different sets of samples. Samples from the sets 1 and 2 gave rather weak signals compared to those observed in the samples from sets 3 and 4. The difference in the concentration of the Si-NL62 center is correlated to the creation ability of the new centers Si-NL63 and Si-NL64, to be described in the following paragraphs. Spectrum A23 of the Au-Fe center is observed in all gold-doped *n*-type samples, in *p*-type material only after additional hydrogenation. Its spin concentration, estimated at 10^{14} to 10^{15} cm^{-3}, depends on preparation conditions. Figure 1 shows the Au-Fe concentration to be smaller than NL62, whereas, after hydrogenation, see Fig. 5, the concentration is two orders of magnitude larger. The Au-Fe concentration also increases during room temperature sample storage.

B. EPR spectrum Si-NL63

The same samples in which the Si-NL62 center is present were subjected to a further heat treatment in which hydrogen is uniformly introduced throughout the sample volume by diffusion, as described. Following this processing step, a new EPR spectrum, labeled Si-NL63, is observed. Figure 5 shows the spectrum, simultaneously present with the spectrum Si-NL62 in a similar concentration and the much stronger Au-Fe pair.

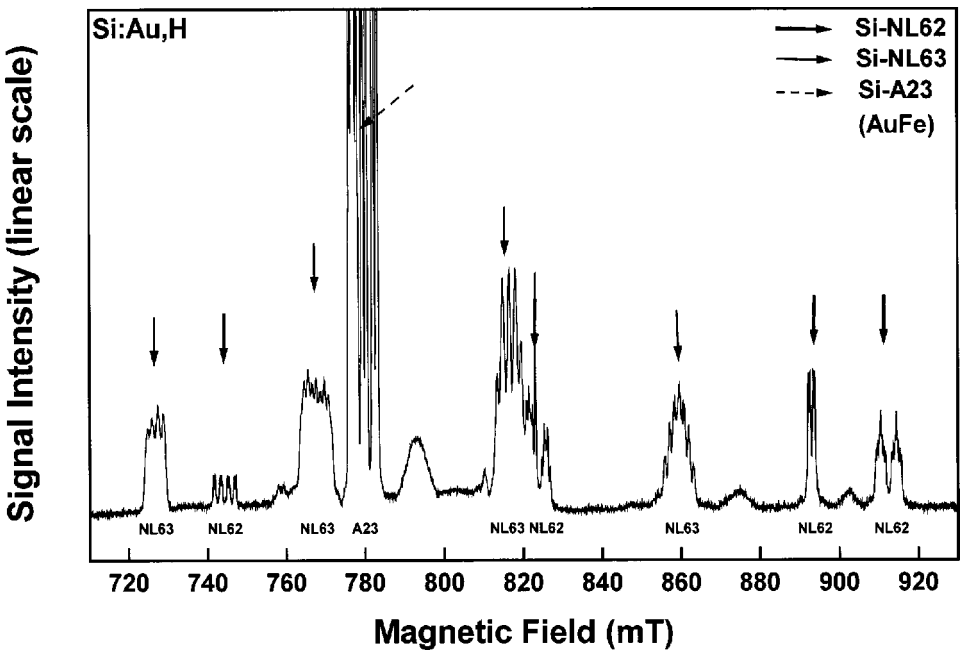

FIG. 5. EPR spectra observed after gold doping and hydrogenation for a wide range of magnetic field, with direction of **B** about 1° away from the [011] crystallographic direction. Microwave frequency $\nu=23.0217$ GHz, temperature $T=4.2$ K. The observed spectra Si-NL62, Si-NL63, and Si-A23 of Au-Fe are indicated by bold, solid, and dashed arrows, respectively.

Also spectrum Si-NL63 has monoclinic-I symmetry, as indicated by the angular rotation shown in Fig. 6. Principal g values following from the pattern are given in Table I. Spectrum Si-NL63 is exceptional by its complex hyperfine structure. Spectral lines with a typical width of 0.7 mT are about four times broader than line widths of the Si-NL62 center. Characteristic hyperfine structures are observed in the principal directions of the center. For $\mathbf{B}\|[011]$, i.e., for the resonance in the g_1 direction, seven equidistant components with the typical intensity ratio 1:2:3:4:3:2:1, as shown in Fig. 7, are observed on the orientations *bc* and *cb*. Such a structure, composed of a total of 16 transitions, cannot be explained with a single $I=\frac{3}{2}$ nucleus of gold. On the other hand, the structure is easily explained as the superposition of spectra of two equivalent $I=\frac{3}{2}$ nuclei, i.e., gold, and is usually taken as its unambiguous fingerprint. In other directions the spectrum is collapsed into four lines with equal distance and intensity, as shown in Fig. 8 for orientations *ad* and $(bd+cd)$ in a deuterated sample. While this would be typical for a one-gold center, the structure is hard to explain by two such atoms on symmetry-related positions. Assuming, as usually

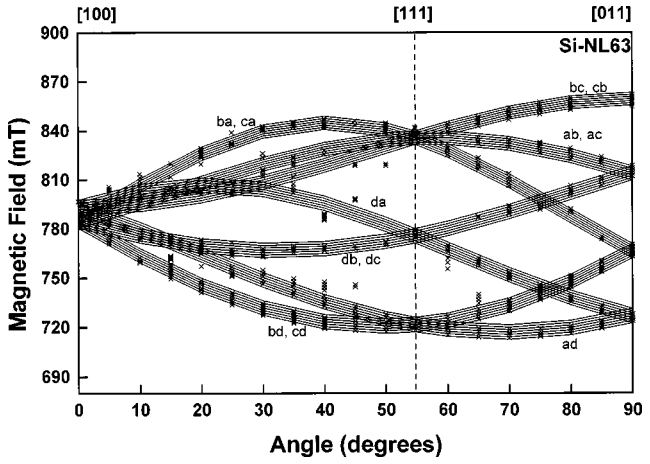

FIG. 6. Monoclinic-I angular dependence pattern of the Si-NL63 spectrum for rotation of the magnetic field in the $(0,-1,1)$ plane from [100] to [011]. Experimental data recorded at temperature $T=4.2$ K for microwave frequency $\nu=23.0217$ GHz are presented by $\times$. Solid lines are from the computer fit using the spin Hamiltonian of Eq. (1) without quadrupole interaction ($\mathbf{Q}=0$). Labeling of the defect orientations is indicated.

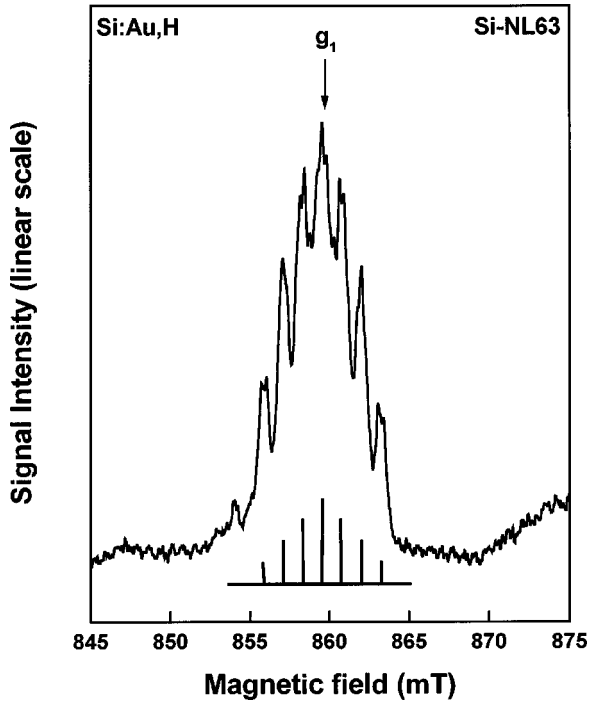

FIG. 7. EPR spectrum Si-NL63 recorded in the principal direction $\mathbf{B}\|[011]$ on defect orientations $(bc+cb)$. The typical line structure with seven equidistant lines with the intensity ratio 1:2:3:4:3:2:1 is indicated by stick diagram.

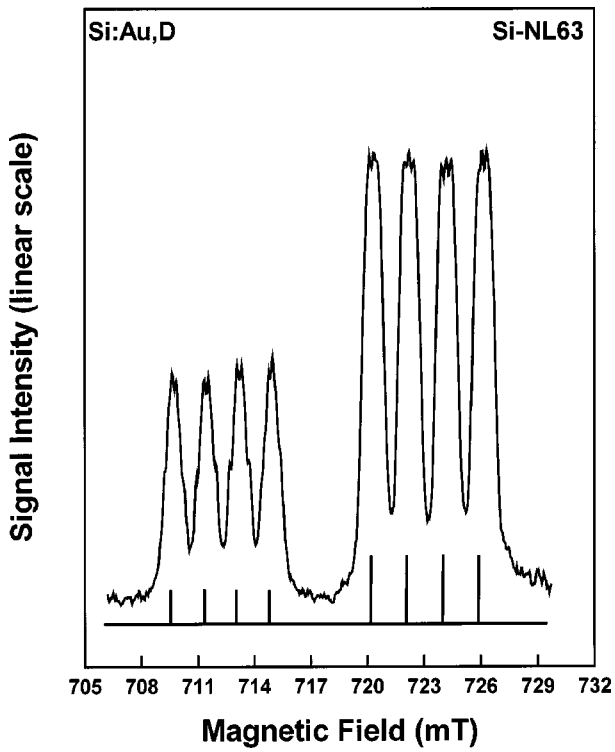

FIG. 8. EPR spectrum of the Si-NL63 center showing the effect of deuterium substitution on defect orientations *ad* and $(bd+cd)$. Magnetic field is in the $(0,-1,1)$ plane at an angle of 20° away from [011]. The typical line structure of four lines at equal distance and intensity ratio as 4:4:4:4 is observed.

correct for gold centers, a large quadrupole effect, there is an abundance of normally forbidden transitions which become allowed and which can actually dominate the spectrum, but their number is likely to be large and odd, contrasting to the observed four. In a similar case, in the analysis presented for the two-gold center LAu2 no four-line spectra occur.[30] In an alternative model, offering more matching parameters, a center with one gold atom plus an additional impurity also with a nuclear spin $I=\frac{3}{2}$ can be considered. Suitable candidates for this additional impurity are a second inequivalent gold atom, and ^{63}Cu, ^{65}Cu, or ^{11}B atoms. Although for general directions of magnetic field a more complex hyperfine structure is observed, in no case of defect orientation and direction of magnetic field a line structure is met which can be decomposed as a superposition of two hyperfine quartet structures with a different splitting. In view of all observations, our preference is still for a model incorporating two gold atoms on symmetry-related sites. We have not succeeded in finding a unique and convincing match to these data rigorously based on a spin Hamiltonian. In that respect, the hyperfine parameters given in Table I and the fitting curves in Fig. 6 should be considered as indicative.

To further examine the relation to gold, the formation of the spectrum Si-NL63 was quantitatively monitored in the samples from sets 1 to 4. In samples with a low concentration of gold, those from sets 1 and 2, after hydrogenation only the Si-NL62 spectrum is detected, no Si-NL63 nor other centers. Spectrum Si-NL63, and another spectrum Si-NL64, to be described in Sec. III C, are generated only in the gold-rich samples of sets 3 and 4. This evidence relating the formation of the Si-NL63 center to the presence of gold in higher concentration supports the pair model.

Following from its formation conditions, the presence of hydrogen in the Si-NL63 structure is expected. Hyperfine interaction with hydrogen often has a strength of 10 MHz, corresponding to splittings in the EPR of 0.3 mT. Structure of such a magnitude is abundantly observable and determines the line shapes of Si-NL63 resonances as shown in Fig. 7. The hydrogen origin is confirmed by replacing hydrogen with deuterium, diffused under the same conditions of time and temperature. A slow scan with optimized resolution, as presented in Fig. 8, shows the different deuterium-related structure. As the resonance lines are broad, the angular dependence could not be followed and interaction tensors not quantitatively be determined. Neither could the number of hydrogen atoms be unambiguously established. However, in view of the rich structure, their number should be from 2 to 4.

C. EPR spectrum Si-NL64

Under visible-light illumination, in the hydrogenated gold-diffused samples, another previously not reported spectrum appeared to be present. The spectrum, labeled Si-NL64, arises from a low-symmetry center with a corresponding large number of fine-structure lines reflecting the orientational degeneracy. As the center is observed in the simultaneous presence of the Si-NL62, Si-NL63, and Au-Fe centers, the complete recorded spectrum is rather full of resonances over a field range less than 100 mT. As a result the angular dependence of the Si-NL64 spectrum is difficult to follow. In the experiment, fortunately, the Si-NL64 spectrum could be enhanced. First, the three centers Si-NL62, Si-NL63, and Si-NL64 are observed under different conditions of field passage and can be optimized individually. Secondly, the intensity of the Si-NL64 spectrum increases in a sensitive way with the level of illumination. Since at the same time the Si-NL62 intensity decreased significantly, the Si-NL64 could be made the dominant spectrum. Thirdly, by a heat treatment of the sample at 150 °C the Si-NL64 spectrum became observable without illumination.

Spectrum Si-NL64 has a clear and informative hyperfine structure. Each fine-structure transition shows as a main feature a fourfold splitting which can be ascribed to the hyperfine interaction with a gold atom. In addition, a threefold splitting of each gold component reveals further hyperfine interaction with two nuclei $I=\frac{1}{2}$, identified as hydrogen atoms. Altogether, the hyperfine structure is a twelve-line group with relative intensities of (1:2:1):(1:2:1):(1:2:1):(1:2:1). Those splittings are all just resolved in EPR as illustrated in Fig. 9 on an expanded field scale. Of course, in the triclinic symmetry of the center, no symmetry-equivalent positions are available for two hydrogen atoms. However, in view of the quite constant hydrogen hyperfine interactions found in a number of independent cases, the assumed equal interaction for two sites does not present a problem in the practical sense. Confirmation of the

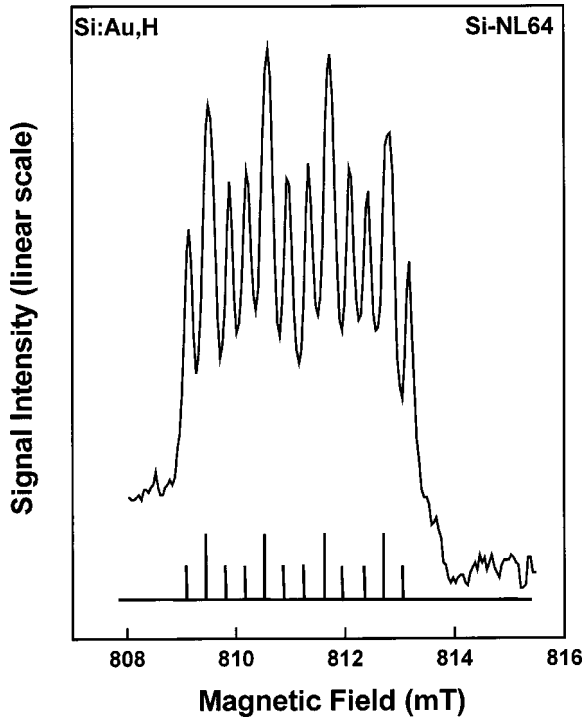

FIG. 9. Part of the EPR spectrum of the Si-NL64 center with clear presence of the hyperfine interaction with one gold and two quasi-equivalent hydrogen atoms, resulting in the structure (1:2:1):(1:2:1):(1:2:1):(1:2:1) of spectral lines. The spectrum is recorded at temperature $T=4.2$ K, with microwave frequency $\nu=23.0217$ GHz, and with magnetic field **B** in the $(0,-1,1)$ plane at an angle about 10° away from [011].

hydrogen identification has been obtained by deuterium substitution. With a nuclear spin $I=1$, the number of hyperfine states will be larger than for the proton. As the deuteron also experiences quadrupole interactions, many more transitions will be possible. As a result, the nuclear structure in the spectrum no longer is resolvable. The clear isotope effect provides direct evidence for hydrogen incorporation in the Si-NL64 center.

An angular dependence pattern of the Si-NL64 center produced under optimized conditions is shown in Fig. 10 and has the unique features of the triclinic symmetry. Quantitative analysis has been performed with the Hamiltonian

$$H=\mu_B \mathbf{B}\cdot\mathbf{g}\cdot\mathbf{S}+\mathbf{S}\cdot\mathbf{A}^{\mathrm{Au}}\cdot\mathbf{I}^{\mathrm{Au}}+\Sigma_{i=1,2}\mathbf{S}\cdot\mathbf{A}_1^{\mathrm{H}}\cdot\mathbf{I}_1^{\mathrm{H}}, \qquad (3)$$

taking into account hyperfine interactions with one gold and two hydrogen atoms. No quadrupole energy was invoked. In view of overlap of the Si-NL64 resonances with the Au-Fe spectrum, the experimental data points in the magnetic field range 775 to 780 mT are omitted. The experimental data show a good coincidence with the simulated angular dependence using the spin Hamiltonian of Eq. (3). Parameters determined by fitting are given in Table I.

IV. DISCUSSION

A. Center Si-NL62

In all models of gold and gold-related centers in silicon, the gold impurity is concluded to be on a substitutional site,

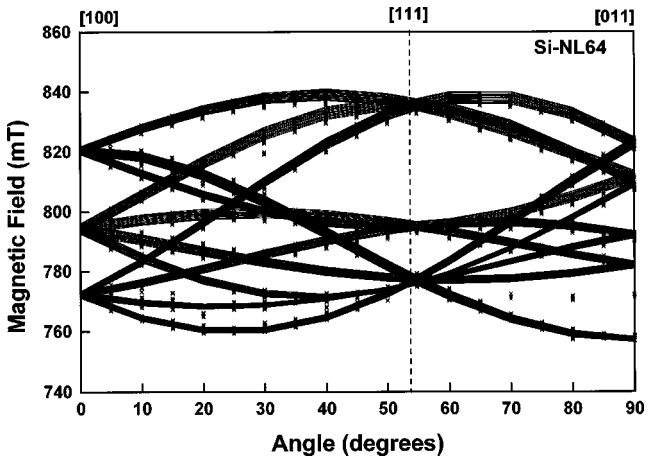

FIG. 10. Triclinic angular dependence pattern of the Si-NL64 spectrum for rotation of the magnetic field in the $(0,-1,1)$ plane from [100] to [011]. Experimental data recorded at temperature $T=4.2$ K for microwave frequency $\nu=23.0217$ GHz are presented by $\times$. Solid lines represent simulation of the spectrum using the spin Hamiltonian of Eq. (3) and parameters of Table I.

forming the core atom in a silicon vacancy. In the bonding between gold and surrounding silicon atoms issues of interest are the symmetry of the resulting defect structure and the distribution of electrons over the defect site. From theoretical calculations by Lowther and Fazzio *et al.* the isolated substitutional gold atom in silicon tends to bond with two silicon atoms, with the bonds on the other two atoms of the vacancy site reconstructed.[1–3] The model results in an amphoteric two-level system with three charge states of the gold atom possible.[3,5,6] With a Fermi level above the donor state at $E_v+0.35$ eV and below the acceptor state at $E_c-0.55$ eV, the neutral defect is paramagnetic and an obvious candidate for observation by EPR.

Experimentally, an unambiguous interpretation for the atomic configuration and electronic structure of neutral substitutional gold in silicon has been presented. From Zeeman studies of the donor and acceptor excitation spectra at 793 and 611 meV, Watkins *et al.* have concluded that the neutral isolated gold center is paramagnetic, is described by electron spin $S=\frac{1}{2}$, and has an axial **g** tensor with $g_{\parallel[100]}\approx 2.8$ and $g_{\perp[100]}\approx 0$, corresponding to a static tetragonal distortion.[31] The fact that $g_{\perp}\approx 0$ prevents the EPR detection of Au^0.

For a theoretical interpretation the vacancy model, following Watkins' early proposal,[33] was developed into a quantitative model,[34,35] and provides the most powerful tool for analysis of data. For the present application to the Si-NL62 center reference is made to these papers for the definition of quantities and the meaning of symbols. The electron state is described as a linear combination of t_2 gap states of the vacancy and d states of the gold atom. Normalized wave function coefficients are given as u, v, and w, with $u^2+v^2+w^2=1$. The relative localization on the gold atom is N^2. Deviation of the g value from its free-electron value $g_e=2.0023$ will be due to admixture of orbital angular momentum which is attributed to the heavy gold atom only. Taking into account the opposite sign of matrix elements in the effective spin for the triplet, the orbital g factor is $g_L=-N^2$.

Solving for the eigenvalues of the Zeeman Hamiltonian, the g tensor has the following principal values:

$$g_{xx}=g_e(2uv-w^2)-2\sqrt{2}g_L w(u-v), \tag{4}$$

$$g_{yy}=g_e(2uv+w^2)+2\sqrt{2}g_L w(u+v), \tag{5}$$

and

$$g_{zz}=g_e(1-2w^2)-2g_L(u^2-v^2). \tag{6}$$

With the experimental data for the **g** tensor $g_{xx}=1.8424$, $g_{yy}=1.7165$, and $g_{zz}=2.2435$, the valid exact solution of Eqs. (4) to (6) will give $u=0.83$, $v=0.55$, $w=0.09$, and $g_L=-0.37$. The small value of w reflects the small admixture to the wave function of the higher-lying orbital singlet $|\zeta\rangle$ formed after Jahn-Teller distortion which lifts the degeneracy of the triplet level in the original tetrahedral symmetry. However, the small nonzero value of w with the result that $g_{xx}\neq g_{yy}$ and nonaxial structure of the center and its **g** tensor, allows centers with a near-axial symmetry, such as the present Si-NL62, to be treated. The result $N^2=-g_L=+0.37$ shows a remarkable similarity to the electron localization of the single gold atom, for which, following the simplified treatment of Ref. 35, the localization is found to be $N^2=(g_{\parallel}-2)/(4-g_{\perp}^2)^{1/2}=0.40$. This result implies considerable support for a comparable electronic structure of the two centers.

With the wave function characterized, the hyperfine interactions may as well be considered. The lengthy expressions for the tensor components as given in Ref. 34 will not be reproduced here. On substituting the values calculated for u, v, and w, and putting $g_L=-N^2$, one obtains $A_{xx}=+0.91A_c+16.27N^2$, $A_{yy}=+0.92A_c-98.20N^2$, and $A_{zz}=+0.98A_c+150.59N^2$. To obtain the result, the factor $P=2(\mu_0/4\pi)\mu_B g_n\mu_n\langle r^{-3}\rangle_{5d}/h$ for orbital magnetism on the gold atom has been taken as $P=132$ MHz.[36] Parameter A_c accounts for the, nearly isotropic, core polarization. On comparing with the measured data, one must realize that in the experiments signs of hyperfine constants are not determined. With the help of the above theoretical result, one can conclude that A_{zz} will be the largest value, and A_{yy} the smallest. Taking account of this indication, the experimental values are taken as $A_{xx}=-31.4$ MHz, $A_{yy}=-65.7$ MHz, and $A_{zz}=+57.5$ MHz. A best match with the data from experiment is then obtained for $A_c=-25.34$ MHz and $N^2=+0.48$. For these values of A_c and N^2 the calculated hyperfine constants become $A_{xx}=-15.2$ MHz, $A_{yy}=-70.2$ MHz, and $A_{zz}=+46.8$ MHz. Given the approximations in the theoretical treatment, and also the fact that u, v, and w parameters as obtained from **g**-tensor analysis were used without any further optimization, the result should be considered as quite satisfactory. Parameter A_c has an expected negative value with a comparable magnitude to core polarizations calculated for Au-Li and Au-Li_3 centers.[37,38] Decomposing the hyperfine tensor into its isotropic part a and anisotropic part b in an axial approximation, one obtains $a=(1/3)(A_{xx}+A_{yy}+A_{zz})=-13.2$ MHz and $b=(1/6)(2A_{zz}-A_{xx}-A_{yy})=+35.4$ MHz. Relating the anisotropic part to the gold $5d$ orbitals in the common LCAO analysis, an occupation $\eta^2\beta^2=0.94$ is calculated. This could easily lead to a conclusion of almost a full hole in the d shell of gold, in a strong contradiction to the basic idea behind the vacancy model. The discrepancy with the earlier result for N^2 can, however, be traced to be due to neglect of orbital interaction in the LCAO treatment, which can lead to substantial errors, such as, e.g., demonstrated in the calculations for the Au-Li and Au-Li_3 centers.[37,38]

Analyzing the **A** tensor in its full anisotropic form, after subtraction of the isotropic matrix $a.\mathbf{1}$, the anisotropic traceless tensor **B** has components $b_{xx}=-18.2$ MHz, $b_{yy}=-52.5$ MHz, and $b_{zz}=+70.7$ MHz. One notices that $b_{yy}/b_{xx}=+2.9$ and $b_{zz}/b_{xx}=-3.9$, showing a good correspondence to the ratio's as derived for the quadrupole tensor $q_{yy}/q_{xx}=+4.2$ and $q_{zz}/q_{xx}=-5.2$. Both hyperfine and quadrupole parameters are related to the occupancy of the gold $5d$ orbitals. Components are given, respectively, by

$$b=\eta^2\beta^2(2/7)(\mu_0/4\pi)g\mu_B g_n\mu_n\langle r^{-3}\rangle_{5d}, \tag{7}$$

$$q=\eta^2\beta^2(2/7)(1/4\pi\varepsilon_0)[e^2Q/2I(2I-1)]\langle r^{-3}\rangle_{5d}, \tag{8}$$

and are, therefore, related by

$$q/b=e^2Q/2I(2I-1)\varepsilon_0\mu_0\mu_B g_n\mu_n. \tag{9}$$

Substituting the physical parameters for the ^{197}Au isotope, $I=\frac{3}{2}$, $g_n=0.09717$, and $Q=0.59\times10^{-28}$ m^2, the ratio q/b is calculated as 2.51. The result supports the earlier assumption of large quadrupole effects on the spectrum, which is an established specific feature for gold following from its unusually small g_n factor and large quadrupole moment Q. With $q/b=2.51$ the quadrupole component for the Si-NL62 center is estimated at $q=(1/6)(2q_{zz}-q_{xx}-q_{yy})=90$ MHz. One electron is therefore held responsible for both the unpaired spin density and the charge unbalance in the center. It is also concluded that all three tensors **g**, **A**, and **Q**, have a near-axial symmetry along a common axis.

In addition to gold, the ligand hyperfine interaction with ^{29}Si was also observed in the experiment and associated with two neighbor atoms. In the vacancy model the electron distribution over the neighbor pairs, labeled (a), (d) and (b), (c), is given by $p_{ad}=(\frac{1}{2})(u+v)^2$ and $p_{bc}=(\frac{1}{2})(u-v)^2$. With the numerical values for u and v substituted, these occupation ratio's become $p_{ad}=0.96$ and $p_{bc}=0.04$. The orbital on the a and d atoms strongly predominates over the orbital between the b and c atoms, consistent with the experimental observation of hyperfine interaction with only two of four silicon neighbors. In experiment the isotropic part of ^{29}Si hyperfine interaction is determined as 110 MHz, corresponding to an s-type density $\alpha^2\eta^2=2.2\%$. When accepting a real orbital of hybridized sp^3-type the neighbor bonds a and d could each account for as much as 8.8% of an electron. With the estimated $N^2\approx40\%$ for the localization on gold the description of a molecular orbital constructed from gold states and four vacancy neighbors does not fully cover the whole region of electron distribution.

Following from the discussion, the Si-NL62 center is concluded to be a one-gold center. On the basis of experimental characterization an equal conclusion has been drawn earlier

for the Si-NL50 center[39] and for a center observed in optical Zeeman spectroscopy,[31] to which it became customary to refer to just as single substitutional gold. In this difficult situation where three spectra are the competitive candidates for one center, brief arguments pro and con can be presented as follows. Whereas the Si-NL62 center shows distortions leading to the observed low monoclinic symmetry, there are no other indications of strong perturbations of its electronic structure, e.g., by the formation of a gold-impurity complex. Any hyperfine interaction with an additional impurity is absent in the spectra, which, together with the high purity of the materials used, strongly reduces the available options. This leaves open the possibility of accommodation of the gold atom in an intrinsic defect, such as the vacancy or a larger defect. The divacancy with monoclinic symmetry in both positive and negative charge states is a suitable candidate. All the same discussion as for the spin-Hamiltonian parameters of spectrum Si-NL62 applies to the C_{1h} spectrum as well, with the conclusion that the two associated centers must be very similar, if not identical.[29] The orthorhombic EPR center Si-NL50, another one-gold center without any observed other component, has also been considered as the single substitutional gold center.[39] In recent experiments the formation of Au_sFe_i pairs was observed with a simultaneous one-to-one decrease of the intensity of the Si-NL50 spectrum. A reaction in which the single substitutional gold, monitored by its Si-NL50 EPR spectrum, is lost by complexing with one iron atom, a well-established process, is an almost compelling model. The Au_sFe_i center, with EPR spectrum A23, is firmly identified as the complex of one substitutional gold atom and one interstitial iron atom. The **g** tensor of the NL50 does not lend itself to analysis within the vacancy model. Strong evidence in favor of the center observed in Zeeman optical spectroscopy,[31] has also been presented. Especially the ability of this center to reorient at low temperature is evidence of the absence of any locking field related to a nearby impurity. Being observed in optical spectroscopy, with no hyperfine structure revealed, the identification of the observed impurity in such spectra is based on indirect evidence. In spite of the large amount of available data, the final modeling of the three centers requires more experimental and theoretical studies.

B. Center Si-NL63

As described in the experimental Sec. III B, the Si-NL63 center is only formed after hydrogenation/deuteration of the samples from sets 3 and 4 with high gold concentration and strong presence of the Si-NL62 center. The participation of one gold atom is suggested by the hyperfine structure 4:4:4:4 as observed for defect orientations ad and $(bd+cd)$, illustrated by Fig. 8. In spite of this evidence, the conclusion towards one gold atom is not adopted. In other directions, see, e.g., Fig. 7, a line structure 1:2:3:4:3:2:1 is observed. Although these 16 transitions could be understood as the observation of all transitions between the upper four $|+1/2,m_I\rangle$ levels and the lower four $|-1/2,m_I\rangle$ levels, this would require equal probability of four allowed and twelve forbidden transitions. Also, the equal distance between resonance lines would be difficult to reconcile. For large quadrupole effect, the four levels for each m_S separate into two doublets, at about the energy $+3Q_{\text{eff}}$ for the states $m_I=\pm\frac{3}{2}$ and around energy $-3Q_{\text{eff}}$ for the states $m_I=\pm\frac{1}{2}$. This leads to a spectrum with an intensity structure 4:8:4 at energies $+6Q_{\text{eff}}$, 0, and $-6Q_{\text{eff}}$, respectively. Finally, the **g** tensor of center Si-NL63 does not lend itself to analysis within the vacancy model. The conclusion toward two gold atoms in the center is therefore strongly raised for the discussion. As the given spectra are characterized by equidistant lines, the gold atoms are most likely on symmetry-equivalent lattice sites.

Homonuclear impurity pairs are by no means exceptional complexes in silicon. Such defect structures have been identified for the transition elements iron,[40,41] copper,[42] silver,[43,44] platinum,[45–47] and also for gold. A gold-gold pair of orthorhombic-I symmetry, the Si-LAu2 center, has been observed in electron paramagnetic resonance.[30] The appearance of a 1:2:1 structure of spectral lines was explained as being the result of two equivalent Au atoms lying in one of the mirrorplanes, on sites symmetrically placed above and below the other mirror plane. The spectrum was also observed in the present experiments under illumination by visible light. Although being formed under similar conditions of gold diffusion and hydrogenation, center Si-LAu2 is distinct from the Si-NL62 spectrum, having different symmetry and **g** tensor.

In optical spectroscopy a different gold pair of trigonal symmetry was identified.[48] On the basis of detailed studies the equivalence of the two gold atoms was established. As a model, a pair of gold atoms inside a divacancy was proposed. This defect might well be the core of the Si-NL63 center. Experiment shows that formation of the Si-NL63 center follows the formation of the Si-NL62 center, and the presence of Si-NL62 might be a strict requirement.

In the previous section, for Si-NL62 a half-filled divacancy was presented as a suitable defect model. From this structure the trigonal optical center can be formed by the subsequent capture of another gold atom taking the position of a neighboring vacant site. With the accommodation of two gold atoms, each with the $5d^{10}6s$ configuration, the analog of a VV^{2-} defect is created, which by itself is not a paramagnetic center. Adding two hydrogen atoms in symmetry-equivalent positions will create a monoclinic-I point-group $2/m$ (C_{2h}) center, which upon ionization becomes paramagnetic. Alternatively, adding three hydrogen atoms, in one (110) plane, will still create a monoclinic defect with a point-group symmetry m (C_v) but with the gold atoms no longer on strictly equivalent positions. The center is paramagnetic when neutral. Some of the options for Si-NL63 modeling are illustrated in Fig. 11(b).

C. Center Si-NL64

For the center Si-NL64, a most attractive feature is the well-resolved hyperfine structure in its EPR spectrum. For all defect orientations and several directions of magnetic field four equally spaced identical groups of lines are observed, each consisting of three equally spaced lines with an inten-

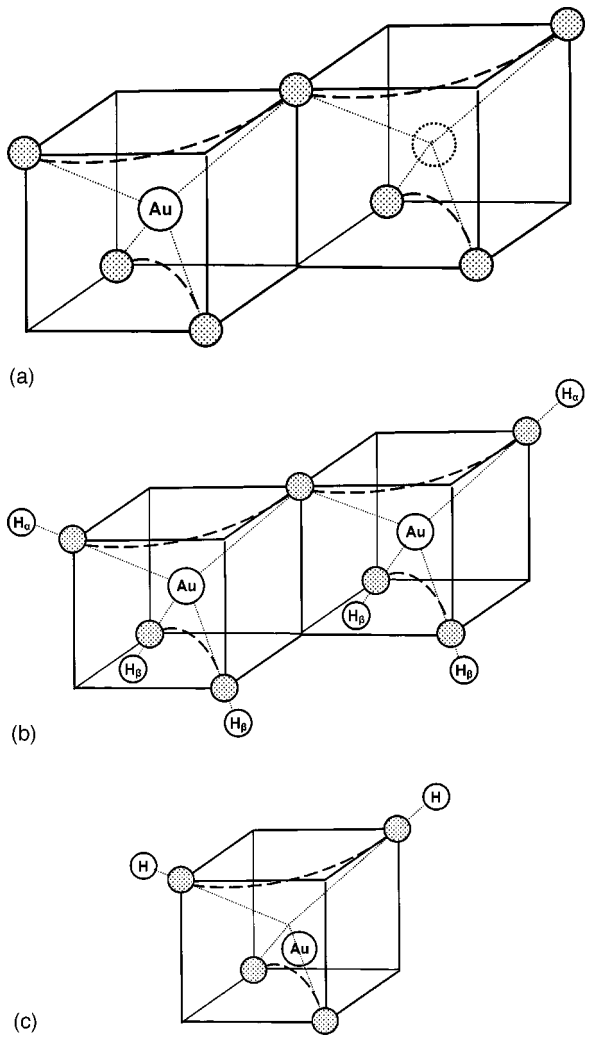

FIG. 11. Atomic models considered for the observed EPR spectra. (a) A single substitutional gold atom together with another lattice vacancy on a (011) plane in monoclinic-I symmetry for center Si-NL62. (b) Two substitutional gold atoms on a common (011) plane for the Si-NL63 center. Sites labeled H_α and H_β allow the decoration of the gold core by two, four, or six hydrogen atoms in the formation of a center with the observed monoclinic-I symmetry. (c) One substitutional gold and two hydrogen atoms for the Si-NL64 center. A spontaneous off-center distortion of the gold atom is required for consistency with the observed triclinic symmetry.

sity ratio 1:2:1. For an illustration, see Fig. 9. In view of the present sample preparation conditions, such a structure forms almost compelling evidence for a center consisting of one gold atom ($I=3/2$, 100%), responsible for the fourfold splitting, and two hydrogen atoms ($I=\frac{1}{2}$, 100%) with an equal hyperfine interaction. For spectrum Si-NL64, in contrast to spectrum Si-NL62, the splitting of resonances by the nuclear interactions always shows a pattern with equal distances between lines. Even though quadrupole effects are almost inevitably present and large, there is no manifestation of them in the recorded spectra. For this reason angular dependencies are analyzed, using Eq. (3), without a quadrupole interaction energy.

As the neutral gold is isoelectronic to negative platinum, a neutral center Au-H_2 could be an atomic and electronic analog of the well-established negative Pt-H_2 center.[24,25,49] Recently, a similar situation was met in the study of lithium complexing with gold and platinum, leading to defects with a comparable trigonal or orthorhombic structure.[37] Hyperfine interaction with the transition metals arises mainly from orbital and dipole-dipole interaction, which both are proportional to the nuclear g factor. As evidenced by the data in Table II, the hyperfine interactions scale corresponding to g_n, which is $g_n=0.09717$ for ^{197}Au and $g_n=1.2190$ for ^{195}Pt. Applying a similar scaling to the hyperfine interactions of Pt-H_2, the values obtained match well with those for the Si-NL64 Au-H_2 center, indicating a similar electronic density. The suggestion on similar electronic structure is firmly supported by the hydrogen hyperfine interactions. For both the gold and platinum centers the isotropic part is found near 10 MHz, corresponding to a very low s-type spin density around 0.7% on the hydrogen position, probably by nearly complete filling of the 1s states by two electrons of opposite spin. Anisotropic hyperfine interaction with hydrogen is due to remote electron spin density, assumed to be mainly present on the gold/platinum site. With parameter $b=1.3$ MHz for the Si-NL64 spectrum and using $b=(\mu_0/4\pi)g\mu_B g_p \mu_n R^{-3}$, the distance $R\approx 0.4$ nm is calculated. With this distance the preferred position of hydrogen is on an antibonding site of a nearest silicon neighbor of the transition metal, an identical result for both the gold and platinum centers.

TABLE II. Comparison of the hyperfine interactions observed for Au- and Pt-related centers with a similar structure. Parameters for Au-H_2 are from the spectrum Si-NL64.

Center	Tensor component	Au	Pt	Ratio Au/Pt
Au/Pt	g_n	0.09717	1.2190	0.0797
Au-Li/Pt-Li	$A_{[011]}$	8.5	118	0.072
Au-Li_3/Pt-Li_3	$A_\parallel$	51.7	696	0.074
	$A_\perp$	36.3	321	0.113
Au-H_2/Pt-H_2	A_1	7.0	175.7	0.040
	A_2	17.7	237.3	0.074
	A_3	30.7	541.2	0.057

Whereas the analysis of hyperfine interactions indicates a strong similarity of the two centers, their overall symmetry is different, as indicated by their **g** tensors. It is not possible to analyze the **g** tensors within the vacancy model, which can be taken as an indication of strong distortion in the core of the center where a vacancy provides room to accommodate the transition metal. The Pt-H_2 center has an orthorhombic-I symmetry, in which the two hydrogen atoms are positioned on symmetry-equivalent sites on an (011) mirrorplane through the platinum atom. For the Au-H_2 center the lower triclinic symmetry suggests to use more flexibility in the positions for gold and hydrogen in modeling the center. This would be allowed as long the distance $R\approx 0.4$ nm is observed. With reference to the model of the Si-NL62 center, it might well be that the low triclinic symmetry is derived by binding two hydrogen atoms to this one-gold center with one hydrogen atom outside the monoclinic mirrorplane. An

atomic model in this spirit is presented in Fig. 11(c). The center is observed in magnetic resonance in its neutral state $[Au_s(H_i)_1(H_i)_2]^0$. If both hydrogen atoms form a center of one negative charge, the gold atom, having transferred two electrons to the stable hydrogen orbitals, has become double positive. With an electron configuration on the gold of $5d^9$ the center is not a good candidate for a treatment in the vacancy model.

Gold-hydrogen centers have also been observed in other experimental studies. Especially in DLTS and the technique of wet chemical etching to introduce hydrogen, several electronic levels due to gold-hydrogen complexes have been reported.[22,23] The actual number of hydrogen atoms in the centers can vary from one to four. In particular for the case of gold, three different electric levels, named G1, G2, and G4, were assigned to one-gold–one-hydrogen complexes. A level G3 was assigned to a one-gold–two-hydrogen complex. By infrared absorption Evans *et al.*[50] observed vibrational modes ascribed to a neutral Au-H_2 center with orthorhombic symmetry, i.e., with features very similar to those observed for the Pt-H_2 defect. These results, though unanimously reporting the binding of hydrogen to gold, platinum, etc., to be an effective process, differ nevertheless still in the details of complexes formed and their activity. Further studies, in which theoretical work on stability, symmetry and electrical activity of centers will play an important role,[51,52] are required for future progress in this field.

V. CONCLUSION

In this paper the atomic and electronic structures of three new paramagnetic centers observed in silicon after doping with gold or gold plus hydrogen/deuterium are discussed. A center labeled Si-NL62 requires the diffusion of gold only and reveals itself in the measurements as a single substitutional gold atom, but in a monoclinic-I environment. It can be characterized by Zeeman interaction **g**, gold hyperfine interaction **A**, and quadrupole interaction **Q** of nearly axial symmetry with axes of the three tensors coinciding. The center is successfully discussed within the vacancy model and then shows almost equal electron localization $N^2 \approx 0.40$ in the $5d$ electron shell of gold as the established single substitutional gold center. Center Si-NL63 has a more complex structure consisting of two, probably equivalent, gold atoms decorated by two, three, or four hydrogen atoms, with all atoms in a monoclinic-I configuration. Hydrogen atoms occupy the common interstitial antibonding sites to a silicon nearest neighbor. The third center, Si-NL64, has one gold and two nearly equivalent hydrogen atoms in a triclinic arrangement. It appeared to be quite similar to the well-studied platinum center Pt-H_2 and the (dis)similarities between the two centers are discussed. In all modeling the idea of accommodating gold atoms in a silicon divacancy has been a leading thought.

[1] J. E. Lowther, J. Phys. C **13**, 3665 (1980).
[2] J. E. Lowther, J. Phys. C **13**, 3681 (1980).
[3] A. Fazzio, M. J. Caldas, and A. Zunger, Phys. Rev. B **32**, 934 (1985).
[4] D. V. Lang, H. G. Grimmeiss, E. Meijer, and M. Jaros, Phys. Rev. B **22**, 3917 (1980).
[5] L.-Å. Ledebo and Z.-G. Wang, Appl. Phys. Lett. **42**, 680 (1983).
[6] J. Utzig and W. Schröter, Appl. Phys. Lett. **45**, 761 (1984).
[7] W. Jost and J. Weber, Phys. Rev. B **54**, R11 038 (1996).
[8] W. Jost, J. Weber, and H. Lemke, Semicond. Sci. Technol. **11**, 22 (1996).
[9] W. Jost, J. Weber, and H. Lemke, Semicond. Sci. Technol. **11**, 525 (1996).
[10] S. Knack, J. Weber, and H. Lemke, Physica B **273–274**, 387 (1999).
[11] N. Yarykin, J.-U. Sachse, H. Lemke, and J. Weber, Phys. Rev. B **59**, 5551 (1999).
[12] N. Yarykin, J.-U. Sachse, J. Weber, and H. Lemke, Mater. Sci. Forum **258–263**, 301 (1997).
[13] J.-U. Sachse, E. Ö. Sveinbjörnsson, W. Jost, J. Weber, and H. Lemke, Phys. Rev. B **55**, 16 176 (1997).
[14] J.-U. Sachse, J. Weber, and H. Lemke, Mater. Sci. Forum **258–263**, 307 (1997).
[15] J.-U. Sachse, J. Weber, and E. Ö. Sveinbjörnsson, Phys. Rev. B **60**, 1474 (1999).
[16] J. Weber, *Hydrogen in Semiconductors and Metals* (Materials Research Society, Warrendale, PA, 1998), p. 345.
[17] S. J. Pearton and A. J. Tavendale, Phys. Rev. B **26**, 7105 (1982).
[18] E. Ö. Sveinbjörnsson, G. I. Andersson, and O. Engström, Phys. Rev. B **49**, 7801 (1994).
[19] E. Ö. Sveinbjörnsson and O. Engström, Phys. Rev. B **52**, 4884 (1995).
[20] E. Ö. Sveinbjörnsson, S. Kristjansson, O. Engström, and H. P. Gislason, *Defect and Impurity Engineered Semiconductors and Devices* (Materials Research Society, Pittsburgh, PA, 1995), p. 371.
[21] E. Ö. Sveinbjörnsson and O. Engström, Mater. Sci. Eng. B **36**, 192 (1996).
[22] L. Rubaldo, P. Deixler, I. D. Hawkins, J. Terry, D. K. Maude, J.-C. Portal, J. H. Evans-Freeman, L. Dobaczewski, and A. R. Peaker, Mater. Sci. Eng. B **58**, 126 (1999).
[23] J.-U. Sachse, E. Ö. Sveinbjörnsson, N. Yarykin, and J. Weber, Mater. Sci. Eng. B **58**, 134 (1999).
[24] P. M. Williams, G. D. Watkins, S. Uftring, and M. Stavola, Phys. Rev. Lett. **70**, 3816 (1993).
[25] M. Höhne, U. Juda, Yu. V. Martynov, T. Gregorkiewicz, C. A. J. Ammerlaan, and L. S. Vlasenko, Phys. Rev. B **49**, 13 423 (1994).
[26] M. Höhne, Phys. Status Solidi B **99**, 651 (1980).
[27] R. L. Kleinhenz, Y. H. Lee, J. W. Corbett, E. G. Sieverts, S. H. Muller, and C. A. J. Ammerlaan, Phys. Status Solidi B **108**, 363 (1981).
[28] H. H. Woodbury and G. W. Ludwig, Phys. Rev. **117**, 1287 (1960).
[29] M. Höhne, Phys. Status Solidi B **119**, K117 (1983).
[30] P. M. Williams, P. W. Mason, and G. D. Watkins, Phys. Rev. B **53**, 12 570 (1996).

[31] G. D. Watkins, M. Kleverman, A. Thilderkvist, and H. G. Grimmeiss, Phys. Rev. Lett. **67**, 1149 (1991).
[32] Yu. V. Gorelkinskii and N. N. Nevinnyi, Physica B **170**, 155 (1991).
[33] G. D. Watkins, Physica B **117–118**, 9 (1983).
[34] F. G. Anderson, F. S. Ham, and G. D. Watkins, Phys. Rev. B **45**, 3287 (1992).
[35] G. D. Watkins and P. M. Williams, Phys. Rev. B **52**, 16 575 (1995).
[36] J. R. Morton and K. F. Preston, J. Magn. Reson. **30**, 577 (1978).
[37] P. Alteheld, S. Greulich-Weber, J.-M. Spaeth, H. Weihrich, H. Overhof, and M. Höhne, Phys. Rev. B **52**, 4998 (1995).
[38] H. Weihrich, H. Overhof, P. Alteheld, S. Greulich-Weber, and J.-M. Spaeth, Phys. Rev. B **52**, 5007 (1995).
[39] N. T. Son, T. Gregorkiewicz, and C. A. J. Ammerlaan, Phys. Rev. Lett. **69**, 3185 (1992).
[40] J. J. van Kooten, E. G. Sieverts, and C. A. J. Ammerlaan, Solid State Commun. **64**, 1489 (1987).
[41] W. Gehlhoff, K. Irmscher, and U. Rehse, Mater. Sci. Forum **38–41**, 373 (1989).
[42] P. N. Hai, T. Gregorkiewicz, C. A. J. Ammerlaan, and D. T. Don, Phys. Rev. B **56**, 4620 (1997).
[43] N. T. Son, T. Gregorkiewicz, and C. A. J. Ammerlaan, J. Appl. Phys. **73**, 1797 (1993).
[44] P. N. Hai, T. Gregorkiewicz, C. A. J. Ammerlaan, and D. T. Don, Phys. Rev. B **56**, 4614 (1997).
[45] H. J. von Bardeleben, D. Stiévenard, M. Brousseau, and J. Barrau, Phys. Rev. B **38**, 6308 (1988).
[46] M. Höhne, Phys. Rev. B **45**, 5883 (1992).
[47] U. Juda and M. Höhne, Solid State Phenom. **47–48**, 293 (1996).
[48] A. Thilderkvist, S. Ghatnekar Nilsson, M. Kleverman, and H. G. Grimmeiss, Phys. Rev. B **49**, 16 926 (1994).
[49] S. J. Uftring, M. Stavola, P. M. Williams, and G. D. Watkins, Phys. Rev. B **51**, 9612 (1995).
[50] M. J. Evans, M. Stavola, M. G. Weinstein, and S. J. Uftring, Mater. Sci. Eng. B **58**, 118 (1999).
[51] R. Jones, A. Resende, S. Öberg, and P. R. Briddon, Mater. Sci. Eng. B **58**, 113 (1999).
[52] R. Jones, B. J. Coomer, J. P. Goss, B. Hourahine, and A. Resende, Solid State Phenom. **71**, 173 (2000).
[53] G. D. Watkins and J. W. Corbett, Phys. Rev. **134**, A1359 (1964).